Int. J. Heat Mass Transfer. Vol. 15, pp. 2119–2132. Pergamon Press 1972. Printed in Great Britain

ON THE HEAT TRANSFER BETWEEN TWO ROTATING DISKS

RAMESH CHANDRA ARORA* and VIJAY KUMAR STOKES†
Department of Mechanical Engineering, Indian Institute of Technology, Kanpur, India

Abstract—Exact numerical solutions of the Navier–Stokes equations have been obtained for the steady state axisymmetric flow of an incompressible Newtonian fluid between two parallel infinite rotating disks, for speed ratios of the two disks varying between -1 and $+1$ in steps of 0·25 and for the Reynolds number varying between 0 and 125. Some representative non-dimensional radial, tangential and axial velocities have been presented graphically.

These velocity profiles have then been used for integrating the energy equation for two sets of boundary conditions: Both the disks kept at constant temperatures and, one disk insulated and the other kept at a constant temperature. The solutions have been obtained for values of the Prandtl number varying between 0·7 and 7·5. The dissipation terms have not been neglected but the properties of the fluid have been assumed to be constant.

Thus, exact numerical solutions have been obtained for the two-disk heat-transfer problem.

NOMENCLATURE

c_p, specific heat of fluid;
D, angular velocity ratio of the disks, Ω_2/Ω_1;
E, Eckert number, $[\Omega_1^2 l^2/c_p(T_1 - T_2)]$;
F_1, F_2, heat transfer to the lower and upper disks repectively;
G, H', H, non-dimensional tangential, radial and axial velocity components respectively;
k, thermal conductivity of fluid;
l, gap width between the rotating disks;
M_1, M_2, torques on the lower ($z = 0$) and upper ($z = l$) disks respectively;
m, n, components of the non-dimensional temperature. Subscripts 1 and 3 are used to indicate their values for problems 1 and 2 respectively;
m_1, $\vartheta_0 m_{11} + m_{12}$;
P, component of non-dimensional pressure;
p, pressure;
R, Reynolds number, $\Omega_1 l^2/\nu$;
r, radial coordinate of cylindrical polar coordinates;
T, temperature of fluid. Subscripts 1 and 2 are used to indicate its value at the lower and upper disks respectively;
u, v, w, radial, tangential and axial components of the velocity respectively;
z, axial coordinate of cylindrical polar coordinates;
ζ, non-dimensional axial coordinate, z/l;
θ, tangential coordinate of cylindrical polar coordinates;
ϑ, non-dimensional temperature, $(c_p/\Omega_1^2 l^2)(T - T_2)$ and $m(\zeta) + \xi^2 n(\zeta)$;
ϑ_0 $(c_p/\Omega_1^2 l^2)(T_1 - T_2)$; 1/E;
Λ, pressure coefficient;
μ, viscosity of fluid;

*Present address: Division of Fluid, Thermal and Aerospace Sciences, Case Western Reserve University, Cleveland, Ohio.

†Present address: Foster-Miller Associates, Inc., 135 Second Avenue, Waltham, Massachusetts 02154.

ν, kinematic viscosity of fluid;
ξ, non-dimensional radial coordinate r/l;
ρ, density of fluid;
σ, Prandtl number, $\mu c_p/k$;
$\tau_{z\theta}$ shear stress component;
Φ, dissipation function;
φ, non-dimensional heat transfer at the lower disk;
ψ, non-dimensional heat transfer at the upper disk;
Ω_1, Ω_2, angular velocities of the lower ($z = 0$) and upper ($z = l$) disks respectively.

1. INTRODUCTION

THIS paper is concerned with the steady state heat transfer between two rotating infinite disks containing an incompressible Newtonian fluid. It is assumed that the fluid properties such as the viscosity and the thermal conductivity are constant; so that the equations of motion are not coupled to the energy equation. The dissipation terms in the energy equations have not been neglected and as such exact numerical solutions to the Navier–Stokes and Energy equations have been obtained.

Two boundary value problems have been discussed: The disks at constant temperatures and, one disk insulated and the other kept at a constant temperature.

Different aspects of the fluid mechanics of the problem have been discussed by Chapple and Stokes [1], Lance and Rogers [2], and Mellor, Chapple and Stokes [3]. Lance and Rogers [2] considered the general case in which both the disks rotate. However, their integration technique is such that the Reynolds number cannot be pre-assigned, so that for different speed ratios of the two disks the solutions come out at different Reynolds numbers. This makes it difficult to compare the velocity profiles for two different speed ratios at the same Reynolds number. The technique used in this paper is a generalization of the method used by Chapple and Stokes [1]. The major limitation of this technique is that it has not been possible to obtain solutions beyond a Reynolds number around 135.

The velocity distributions have been determined numerically for the speed ratios of the two disks varying from -1 to $+1$ at Reynolds numbers up to 125. Some of these velocity profiles have been presented graphically in this paper.

These velocity profiles have then been used to determine the temperature distribution for two sets of boundary conditions for values of the Prandtl number ranging from 0·7 to 7·5. Some representative profiles have been presented graphically. The predicted skin friction and heat transfer at the disks have also been shown graphically. Extensive numerical results and graphical profiles for the velocity distribution and for the heat transfer are available in Arora [4].

2. EQUATIONS OF MOTION

Only axisymmetric steady state solutions are considered. Because of this the continuity equation and the equations of motion in cylindrical polar coordinates (r, θ, z) reduce to

$$\frac{1}{r}\frac{\partial}{\partial r}(ru) + \frac{\partial w}{\partial z} = 0 \tag{1}$$

$$u\frac{\partial u}{\partial r} + w\frac{\partial u}{\partial z} - \frac{v^2}{r} = -\frac{1}{\rho}\frac{\partial p}{\partial r} + \nu\left[\frac{\partial^2 u}{\partial r^2} + \frac{\partial}{\partial r}\left(\frac{u}{r}\right) + \frac{\partial^2 u}{\partial z^2}\right] \tag{2}$$

$$\frac{u}{r}\frac{\partial}{\partial r}(rv) + w\frac{\partial v}{\partial z} = \nu\left[\frac{\partial^2 v}{\partial r^2} + \frac{\partial}{\partial r}\left(\frac{v}{r}\right) + \frac{\partial^2 v}{\partial z^2}\right] \tag{3}$$

$$u\frac{\partial w}{\partial r} + w\frac{\partial w}{\partial z} = -\frac{1}{\rho}\frac{\partial p}{\partial z} + \nu\left[\frac{\partial^2 w}{\partial r^2} + \frac{1}{r}\frac{\partial w}{\partial r} + \frac{\partial^2 w}{\partial z^2}\right]. \tag{4}$$

Assuming the no-slip condition, the boundary conditions for the problem are given by

$$\begin{aligned} &u(r, 0) = 0, \quad v(r, 0) = r\Omega_1, \quad w(r, 0) = 0, \\ &u(r, l) = 0, \quad v(r, l) = r\Omega_2, \quad w(r, l) = 0, \end{aligned} \tag{5}$$

where it has been assumed that the two infinite disks are located at $z = 0$ (lower disk) and $z = l$ (upper disk) and are both rotating about the z axis at angular velocities of Ω_1 and Ω_2 respectively.

It is well known that these equations can be reduced to a set of coupled non-linear ordinary differential equations by the Von Kármán type similarity transformation

$$\begin{aligned} u &= r\Omega_1 H'(\zeta) \\ v &= r\Omega_1 G(\zeta) \\ w &= -2\Omega_1 l H(\zeta) \\ p/\rho &= \Omega_1^2 l^2 P(\zeta) + \tfrac{1}{2}\Lambda\Omega_1^2 r^2 \end{aligned} \tag{6}$$

where $\zeta = z/l$ and l is the gap width between the two disks. The velocity distributions given by equations (6) satisfy the continuity equation (1) identically. H', G and H are essentially the non-dimensional velocities in the r, θ and z directions respectively. Using this transformation, the three equations of motion (2), (3) and (4) reduce to

$$H'''/R = -2HH'' + H'^2 - G^2 + \Lambda \tag{7}$$

$$G''/R = 2H'G - 2HG' \tag{8}$$

$$P' = -2(H''/R + 2HH') \tag{9}$$

where $R = \Omega_1 l^2/\nu$ is the Reynolds number based on the angular velocity of the disk located at $z = 0$ (lower disk). The boundary conditions given by equation (5) reduce to

$$\begin{aligned} &H(0) = H'(0) = H(1) = H'(1) = 0, \\ &G(0) = 1, \qquad G(1) = \Omega_2/\Omega_1 = D. \end{aligned} \tag{10}$$

These six boundary conditions are sufficient for solving equations (7) and (8), in which Λ is an unknown that has to be determined by the boundary conditions. Once G and H have been determined, equation (9) can be integrated to give the pressure distribution.

3. FRICTIONAL TORQUES ON THE DISKS

The component $\tau_{z\theta}$ of the shear stress, giving rise to frictional torques on the disks, is given by

$$\tau_{z\theta} = \mu\frac{\partial v}{\partial z} = \frac{\mu\Omega_1 r}{l}G'(\zeta)$$

so that

$$\tau_{z\theta}(\zeta = 0) = \frac{\mu\Omega_1 r}{l}G'(0)$$

and

$$\tau_{z\theta}(\zeta = 1) = \frac{\mu\Omega_1 r}{l}G'(1).$$

Neglecting end effects, the shear torque M on a disk of radius r is given by

$$M = -\int_0^r \tau_{z\theta} 2\pi r^2 dr.$$

Therefore, the frictional torques M_1 and M_2, on the lower and upper disks respectively, are given by

$$M_1 = -\frac{\pi\mu\Omega_1}{2l}r^4 G'(0)$$

and (11)

$$M_2 = -\frac{\pi\mu\Omega_1}{2l}r^4 G'(1).$$

Thus $-G'(0)$ and $-G'(1)$ give the non-dimensional torque on the lower and upper disks respectively.

4. ENERGY EQUATION

For this case of incompressible, steady axisymmetric flow, the energy equation for the temperature distribution $T(r, z)$ is given by

$$\rho c_p\left(u\frac{\partial T}{\partial r} + w\frac{\partial T}{\partial z}\right) = k\left\{\frac{1}{r}\frac{\partial}{\partial r}\left(r\frac{\partial T}{\partial r}\right) + \frac{\partial^2 T}{\partial z^2}\right\} + \mu\Phi \tag{12}$$

where

$$\begin{aligned} \Phi = 2&\left\{\left(\frac{\partial u}{\partial r}\right)^2 + \left(\frac{u}{r}\right)^2 + \left(\frac{\partial w}{\partial z}\right)^2\right\} \\ &+ \left(\frac{\partial v}{\partial r} - \frac{v}{r}\right)^2 + \left(\frac{\partial v}{\partial z}\right)^2 + \left(\frac{\partial w}{\partial r} + \frac{\partial u}{\partial z}\right)^2. \end{aligned} \tag{13}$$

The partial differential equation (12) can be reduced to ordinary differential equations by the similarity transformation

$$\vartheta(\xi, \zeta) = m(\zeta) + \xi^2 n(\zeta) \tag{14}$$

where

$$\vartheta(\xi, \zeta) = \frac{c_p}{\Omega_1^2 l^2}(T - T_2) \tag{15}$$

is the non-dimensional temperature. Substituting in equation (12) for T from equations (14) and (15) and for u, v and w from equations (6), it follows that m and n satisfy the ordinary linear differential equations

$$m'' + 2\sigma RHm' = -12\sigma H'^2 - 4n \tag{16}$$

$$n'' + 2\sigma R(Hn' - H'n) = -\sigma(G'^2 + H''^2). \tag{17}$$

Subscripts 1 and 3 will be used on ϑ, m and n to indicate their values for problems 1 and 2 respectively.

Problem 1: Upper ($z = l$) and lower ($z = 0$) disks kept at temperatures T_2 and T_1 respectively.

For this problem $\vartheta(\xi, \zeta)$ is written as

$$\vartheta_1(\xi, \zeta) = \frac{c_p}{\Omega_1^2 l^2}(T - T_2). \tag{18}$$

so that the boundary conditions $T(r, 0) = T_1$ and $T(r, l) = T_2$ give

$$\vartheta_1(\xi, 0) = \vartheta_0 = \frac{c_p}{\Omega_1^2 l^2}(T_1 - T_2) = \frac{1}{E} \tag{19}$$

and $\vartheta_1(\xi, 1) = 0$

where $E = \Omega_1^2 l^2 / c_p(T_1 - T_2)$ is the Eckert number.

The boundary conditions on m and n are then

$$m_1(0) = \vartheta_0 = \frac{1}{E} = \frac{c_p}{\Omega_1^2 l^2}(T_1 - T_2), \quad m_1(1) = 0,$$

$$n_1(0) = n_1(1) = 0. \tag{20}$$

The boundary condition $m_1(0) = \vartheta_0 = 1/E$ is rather inconvenient as it requires that the equation for m be solved for each value of ϑ_0. Since equation (16) is linear, this difficulty may be overcome by splitting the solution m_1 into two parts m_{11} and m_{12} such that

$$m_1(\zeta) = \vartheta_0 m_{11}(\zeta) + m_{12}(\zeta) \tag{21}$$

where $m_{11}(\zeta)$ is a solution of the homogeneous part of equation (16), namely

$$m''_{11} + 2\sigma RHm'_{11} = 0,$$

subject to the boundary conditions $m_{11}(0) = 1$, $m_{11}(1) = 0$ and, $m_{12}(\zeta)$ is a solution of equation (16) subject to the boundary conditions $m_{12}(0) = m_{12}(1) = 0$.

For the special case when both the disks are at the same temperature T_2, ϑ_0 is zero and the solution is given by $m_1(\zeta) = m_{12}(\zeta)$ and $n_1(\zeta)$.

Problem 2: Lower disk ($z = 0$) insulated and the upper disk ($z = l$) kept at a constant temperature T_2.

For this problem $\vartheta(\xi, \zeta)$ is written as

$$\vartheta_3(\xi, \zeta) = \frac{c_p}{\Omega_1^2 l^2}(T - T_2), \tag{22}$$

so that the boundary conditions $T'(r, 0) = 0$, $T(r, l) = T_2$, or $\vartheta'_3(\xi, \zeta) = 0$, $\vartheta_3(\xi, 1) = 0$ give

$$m'_3(0) = 0, \quad m_3(1) = 0,$$
$$n'_3(0) = 0, \quad n_3(1) = 0. \tag{23}$$

A slightly different version of this formulation was used by Millsaps and Pohlhausen [5] for their study of the single disk heat transfer problem.

5. HEAT TRANSFER AT THE DISKS

Let F_1 and F_2 be the heat transferred from the fluid to the lower and upper disks respectively for a disk radius of r. Then, neglecting end effects,

$$F_1 = 2\pi k \int_0^r \left.\frac{\partial T}{\partial z}\right|_{z=0} r\,dr$$

and (24)

$$F_2 = -2\pi k \int_0^r \left.\frac{\partial T}{\partial z}\right|_{z=l} r\,dr.$$

With $\vartheta(\xi, \zeta) = m(\zeta) + \xi^2 n(\zeta)$, the expressions for heat transfer given by equations (24) reduce to

$$F_1 = \frac{\pi k \Omega_1^2 l^3}{c_p} \xi^2 \left[m'(0) + \frac{\xi^2}{2} n'(0) \right]$$

and (25)

$$F_2 = -\frac{\pi k \Omega_1^2 l^3}{c_p} \xi^2 \left[m'(1) + \frac{\xi^2}{2} n'(1) \right].$$

By defining non-dimensional heat fluxes φ and ψ for the lower and upper disks respectively, by

$$\varphi = \frac{F_1}{(\pi k \Omega_1^2 l^3/c_p)} \cdot \frac{1}{\xi^2}, \quad \psi = \frac{F_2}{(\pi k \Omega_1^2 l^3/c_p)} \cdot \frac{1}{\xi^2}, \tag{26}$$

the expressions for Problem 1 become

$$\varphi_1 = m_1'(0) + \frac{\xi^2}{2} n_1'(0) = \vartheta_0 m_{11}'(0) + m_{12}'(0) + \frac{\xi^2}{2} n_1'(0),$$

$$\psi_1 = -\left[m_1'(1) + \frac{\xi^2}{2} n_1'(1) \right] = -\left[\vartheta_0 m_{11}'(1) + m_{12}'(1) + \frac{\xi^2}{2} n_1'(1) \right], \tag{27}$$

and those for Problem 2 reduce to

$$\varphi_3 = 0,$$

$$\psi_3 = -\left[m_3'(1) + \frac{\xi^2}{2} n_3'(1) \right]. \tag{28}$$

6. NUMERICAL SOLUTIONS OF THE EQUATIONS

The nonlinear coupled ordinary differential equations (7) and (8) were solved numerically for the boundary conditions given by equation (10) by using the technique described in Chapple and Stokes [1]. The linear ordinary differential equations (16) and (17) were then solved by several different methods to ensure accuracy of the solutions. For details of the numerical procedures used, computation time required, effect of the step size and convergence properties, reference is made to Arora [4].

7. RESULTS AND CONCLUSIONS

The non-dimensional frictional torques $-G'(0)$ and $-G'(1)$, acting on the lower and upper disks respectively, are given in Fig. 1. Because of

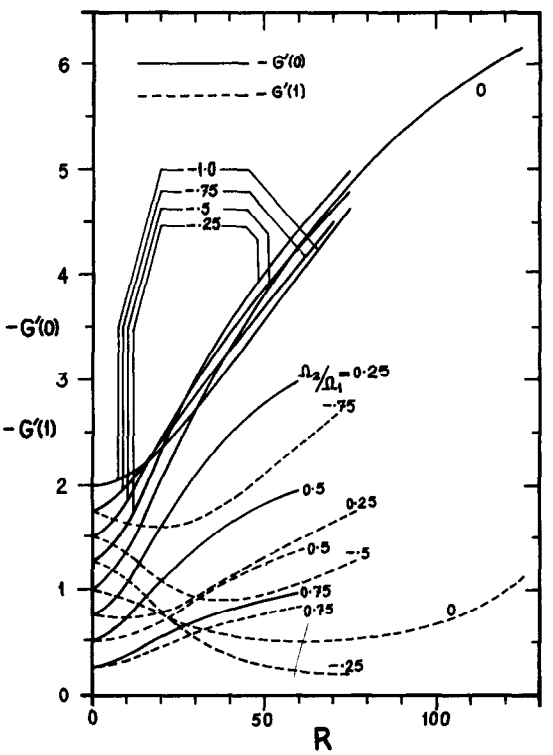

FIG. 1. Variation of the non-dimensional torques $-G'(0)$ and $-G'(1)$ with R for values of D between 0·75 and -1.

symmetry, $G'(0) = G'(1)$ for the special case when $D = \Omega_2/\Omega_1 = -1$. For a Reynolds number of zero, the tangential velocity distribution is given by $G(\zeta) = 1 - (1 - D)\zeta$, so that $-G'(\zeta) = 1 - D$. Thus at $R = 0$, the frictional torque is the same at both the disks. It can be seen that for $R = 0$, the frictional torque is a maximum for $D = -1$ and a minimum for $D = 1$. This trend continues up to about $R = 20$ at both the disks.

At a fixed value of D, the frictional torque at the lower disk increases with increasing Reynolds numbers. On the other hand, at the upper disk, it increases continuously for $D = 0{\cdot}75$, $0{\cdot}5$, $0{\cdot}25$ and -1, shows a minimum for $D = 0$, $-0{\cdot}5$ and $-0{\cdot}75$ and continuously decreases for $D = -0{\cdot}25$ as the Reynolds number increases.

The non-dimensional tangential, axial and radial velocity profiles G, H and H' are shown respectively in Figs. 2–4 for four values of D, namely $0{\cdot}5$, 0, $-0{\cdot}5$ and -1, for both $R = 50$ and $R = 75$. For the case $R = 125$ the velocity profiles have been shown for $D = 0$ only.

When both the disks rotate with the same angular velocity, that is, when $D = 1$, the fluid moves as a rigid body having the same angular velocity as that of the disks, the radial and axial velocities being identically zero. Thus the solution for this case is given by $G(\zeta) = 1$, $H(\zeta) = H'(\zeta) = 0$.

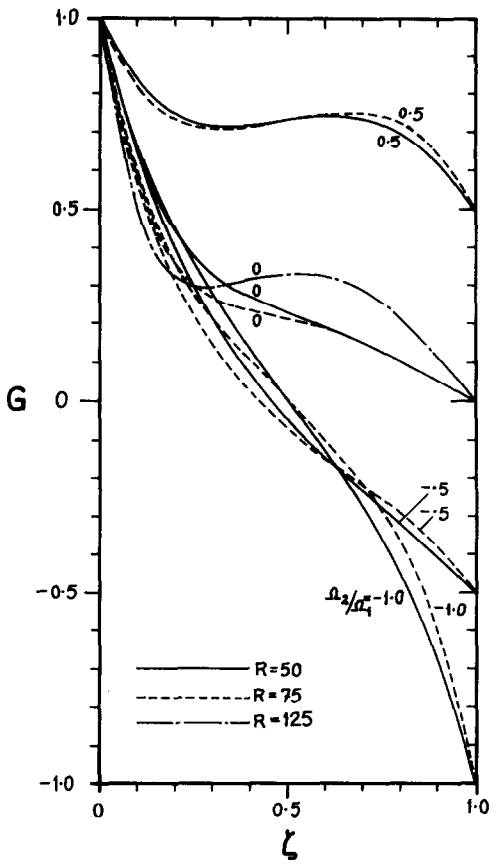

FIG. 2. Variation of the non-dimensional tangential velocity G with ζ.

Tangential velocity (*Fig.* 2)

For a Reynolds number of zero, the tangential velocity varies linearly from one disk to the other. At higher values of the Reynolds number ($R = 75$ and $R = 125$) there is a core which moves as a rigid body, so that the tangential velocity is uniform in the core. For $D > 0$, this phenomenon occurs at lower values of Reynolds numbers as compared to the cases in which $D \leqslant 0$. At still higher values of the Reynolds number, for $D \geqslant 0$, the tangential velocity exhibits an overshoot over the core velocity before settling down to its value at the upper disk.

Axial and radial velocities (*Figs.* 3 *and* 4)

When the disks rotate in the same direction, so that $D \geqslant 0$, the fluid is thrown radially outwards over the faster disk ($\zeta = 0$) while it moves radially inwards at the slower disk ($\zeta = 1$). The axial flow is from the slower to the faster disk.

On the other hand, when the disks rotate in opposite directions (D negative), the fluid is thrown radially outwards at both the disks and moves radially inwards in the core. The axial flow is from the core to both the disks.

For a fixed value of D, the radial velocity increases with increasing values of R. At $R = 75$

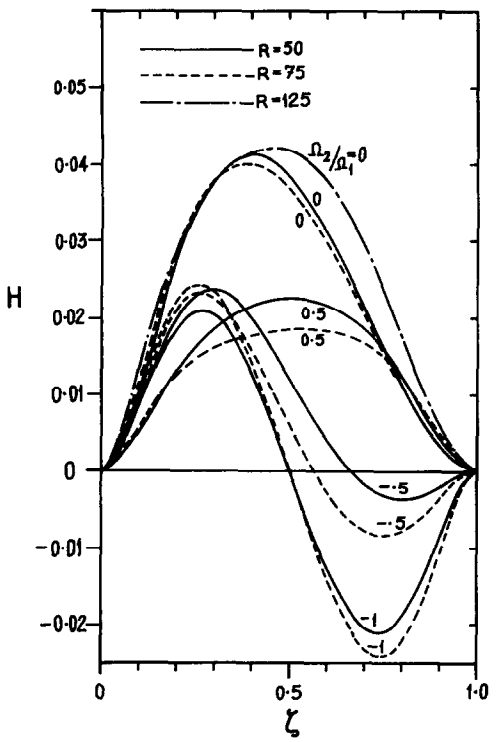

FIG. 3. Variation of the non-dimensional axial velocity H with ζ.

and $D = 0{\cdot}5$, the radial velocity profile exhibits a point of inflection in the vicinity of $\zeta = 0{\cdot}5$. For lower values of D, this phenomenon occurs at comparatively higher values of R. For example, at $D = 0$, the onset of this trend becomes apparent at $R = 125$ only.

At a fixed value of R, the radial outflow and the axial flow towards the faster disk increase as D decreases from 1 to 0, both having a maximum at $D = 0$. As D goes from $-0{\cdot}5$ to -1, these velocity components increase at $R = 75$ and decrease at $R = 50$. The radial outflow at the slower disk ($\zeta = 1$), as well as the axial flow towards it, increase for all values of R as D goes from $-0{\cdot}5$ to -1. As D decreases from 1 to 0, the trend is the same as that at the faster disk.

The major shortcoming of this technique is the fact that it has not been possible to obtain solutions for Reynolds numbers greater than about 135. For high Reynolds numbers one would have to use the methods described by Lance and Rogers [2] and by Mellor, Chapple and Stokes [3]. The limitation of their techniques is that it is not possible to obtain the solutions at prescribed Reynolds numbers without the use of a prohibitive amount of numerical work.

The results for the heat transfer are best described separately for the two problems.

Problem 1: There are two special cases for which closed form solutions exist, namely the limiting case $D = 1$ and the limiting case $R = 0$.

When $D = 1$, the solutions to the equations are given by $m_{11} = (1 - \zeta)$, $m_{12} = 0$ and $n_1 = 0$. Thus the solution is $\vartheta_1 = \vartheta_0(1 - \zeta)$. This is to be expected as for $D = 1$ the fluid has rigid body

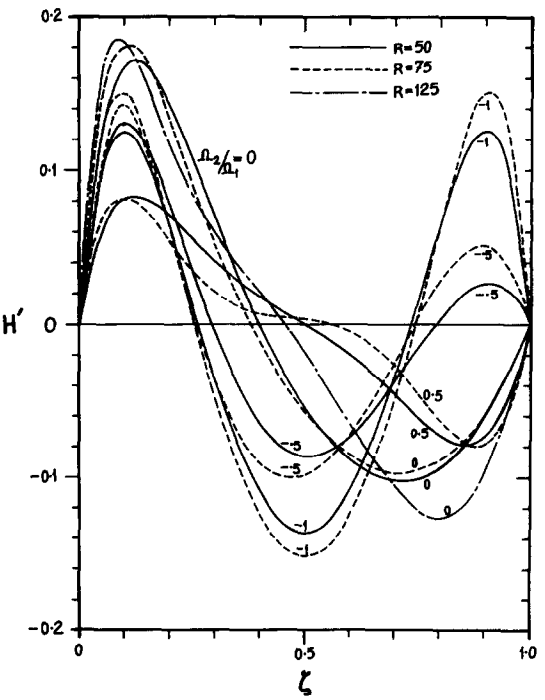

FIG. 4. Variation of the non-dimensional radial velocity H' with ζ.

motion, so that there is no dissipation and the heat transfer is only due to conduction through the fluid.

For the limiting case $R \to 0$, the solution is given by

$$m_{11} = 1 - \zeta$$

$$m_{12} = \frac{\sigma}{6}(1 - D)^2[\zeta - 2\zeta^3 + \zeta^4] \qquad (29)$$

$$n_1 = \frac{\sigma}{2}(1 - D)^2[\zeta - \zeta^2] .$$

Here again, the heat is transferred purely by conduction. However, because of dissipation, the temperature profile is no longer linear and is given by

$$\vartheta_1 = \vartheta_0(1 - \zeta) + \frac{\sigma}{6}(1 - D)^2 \times [\zeta - 2\zeta^3 + \zeta^4 + 3\xi^2(\zeta - \zeta^2)] .$$

The effect of dissipation can be seen in the special case with $T_1 = T_2$ (or $\vartheta_0 = 0$), in which in the absence of dissipation there cannot be any temperature variation. Thus the terms m_{12} and n_1 are both strongly dependent on dissipation. Some representative profiles for m_{11}, m_{12} and n_1 are shown in Figs. 5–7 respectively.

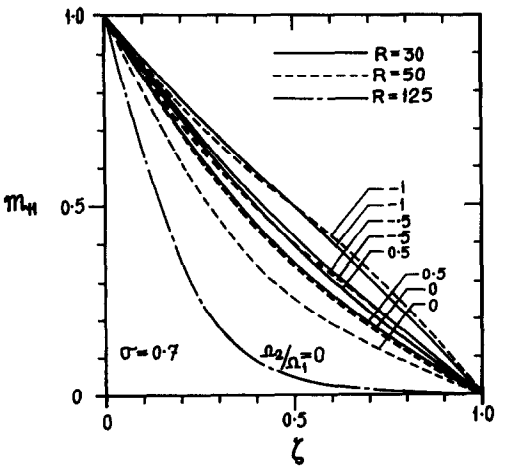

FIG. 5. Variation of the non-dimensional temperature component m_{11} with ζ.

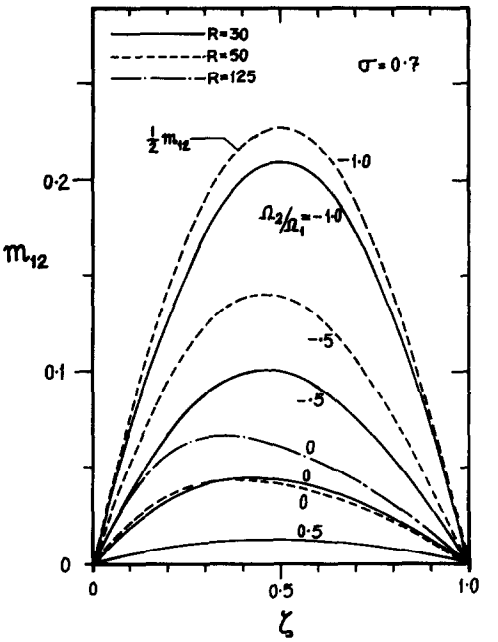

FIG. 6. Variation of the non-dimensional temperature component m_{12} with ζ.

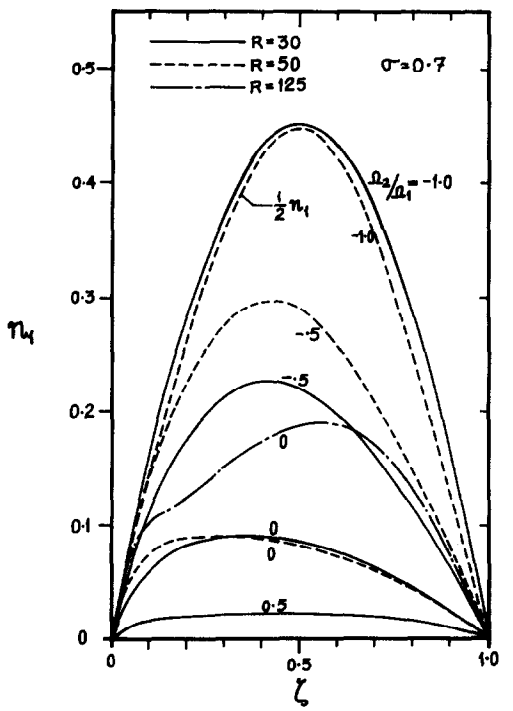

FIG. 7. Variation of the non-dimensional temperature component n_1 with ζ.

The components m_{12} and n_1 being the contributions due to the dissipation of energy, are always positive. Further, the dissipation of energy being a maximum near the disks, gives a boundary-layer character to the profiles of m_{12} and n_1 (see Figs. 6 and 7).

The effect of the Prandtl number on the temperature distribution is shown in Fig. 8 for $R = 10$ and $D = 0$.

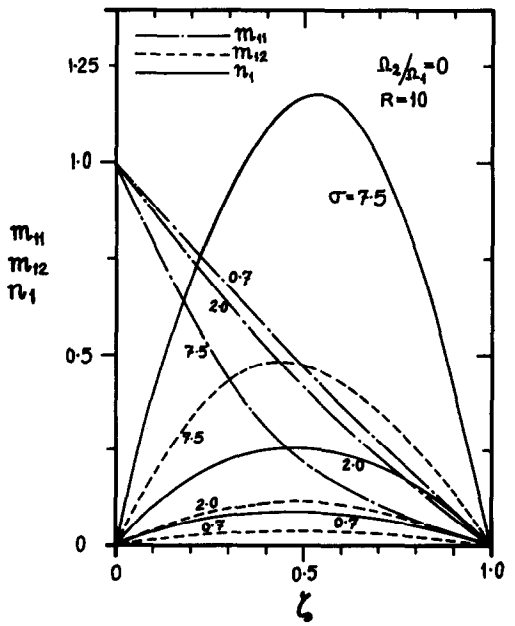

FIG. 8. Effect of the Prandtl number on the temperature components m_{11}, m_{12} and n_1.

With reference to the results of Section 5, especially equations (26) and (27), the heat transfer at the disks can be determined from the information given in Figs. 9–11.

Substituting from equation (29) in equation (27), it follows that the non-dimensional heat fluxes φ_1 and ψ_1 for $R = 0$ are given by

$$\varphi_1 = -\vartheta_0 + \frac{\sigma}{6}(1-D)^2 + \frac{\sigma}{4}(1-D)^2\xi^2$$

and

$$\psi_1 = \vartheta_0 + \frac{\sigma}{6}(1-D)^2 + \frac{\sigma}{4}(1-D)^2\xi^2.$$

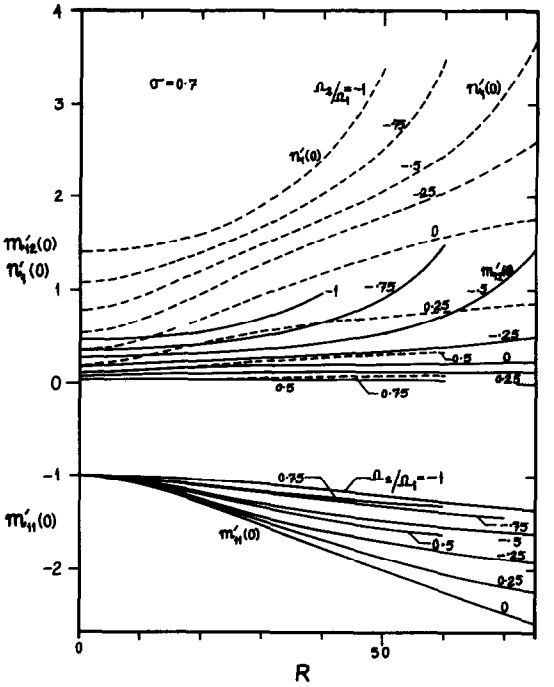

FIG. 9. Variations of the non-dimensional heat flux components $m'_{11}(0)$, $m'_{12}(0)$ and $n'_1(0)$ with R.

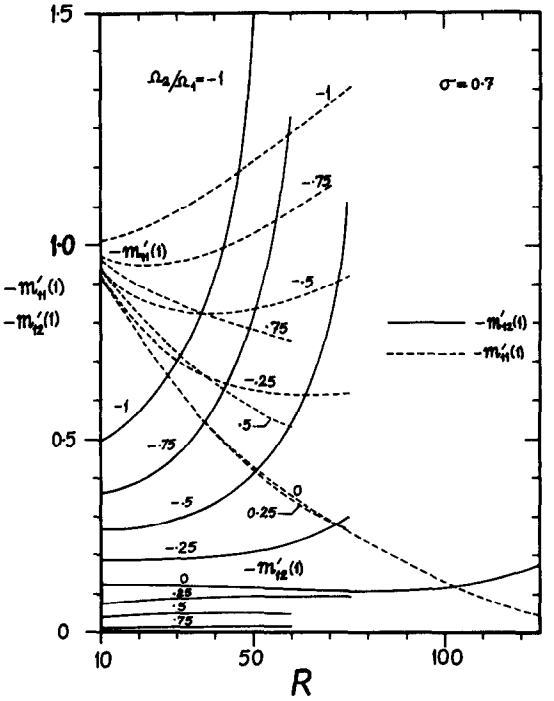

FIG. 10. Variations of the non-dimensional heat flux components $-m'_{11}(1)$ and $-m'_{12}(1)$ with R.

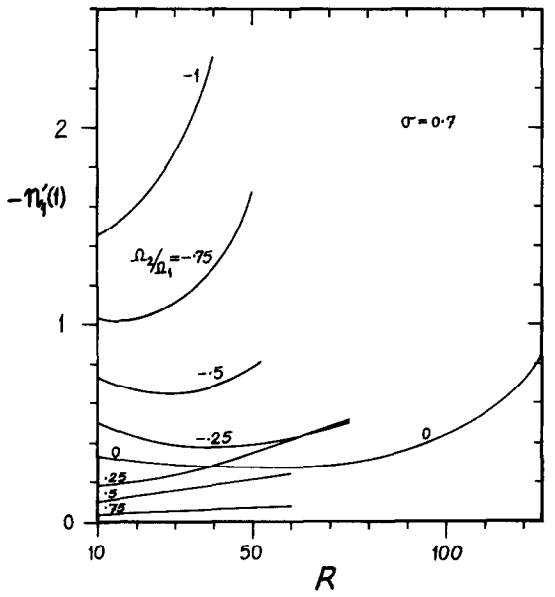

FIG. 11. Variation of the non-dimensional heat flux component $-n_1'(1)$ with R.

If ϑ_0 is assumed to be positive, that is if $T_1 > T_2$, then ψ_1 is always positive whilst φ_1 can change its sign. Just the opposite happens if $\vartheta_0 < 0$. In fact for $\vartheta_0 > 0$, at $\xi = 1$, φ_1 becomes zero when $\vartheta_0 = 1/E = 5\sigma(1 - D)^2/12$. When $\vartheta_0 < 5\sigma(1 - D)^2/12$ or $E > 12/5\sigma(1 - D)^2$, the heat is transferred from the fluid to the lower (hotter) disk. Table 1 shows the values of E for which φ_1 becomes zero at $\xi = 1$, for two values of R.

Thus for a fixed value of R, the Eckert number for which $\varphi_1 = 0$ at $\xi = 1$, increases as D increases from -1 to 1. With increasing values of R and of the Prandtl number σ, the heat flux φ_1 increases but the Eckert number at which $\varphi_1 = 0$ decreases.

Assuming that $T_1 > T_2$, heat is always transferred from the fluid to the upper disk. With increasing values of R, the heat transfer will increase for $D < 0$ and decrease for $D > 0$.

For large diameter disks (ξ^2 much larger than ϑ_0), the heat transfer at the disks will depend mainly on $n_1'(0)$ and $n_1'(1)$ (see equation (27)).

The behaviour of the m and n components of the temperature has been summarized in Table 2.

Table 1. Values of E *for which* φ_1 *becomes zero at* $\xi = 1$

R \ D	−1	−0·75	−0·5	−0·25	0	0·25	0·5	0·75
0	0·86	1·12	1·52	2·19	3·44	6·1	13·7	55
50	0·37	0·60	0·93	1·37	2·24	3·87	7·4	24·8

Table 2. Qualitative behaviour of the m *and* n *temperature components*

Temperature component	Increasing R with D constant: D Positive	Increasing R with D constant: D Negative	D decreases from 1 to 0, R constant	D decreases from 0 to −1, R constant	Increasing Prandtl number, $D = 0$
$m_{11}(\zeta)$	decreases	decreases	decreases	increases	decreases
$m_{12}(\zeta)$	increases	increases	increases	increases	increases
$n_1(\zeta)$	increases	increases	increases	increases	increases
$m_3(\zeta)$	decreases	increases	increases	increases	increases
$n_3(\zeta)$	decreases and overshoots	increases	increases	increases	increases

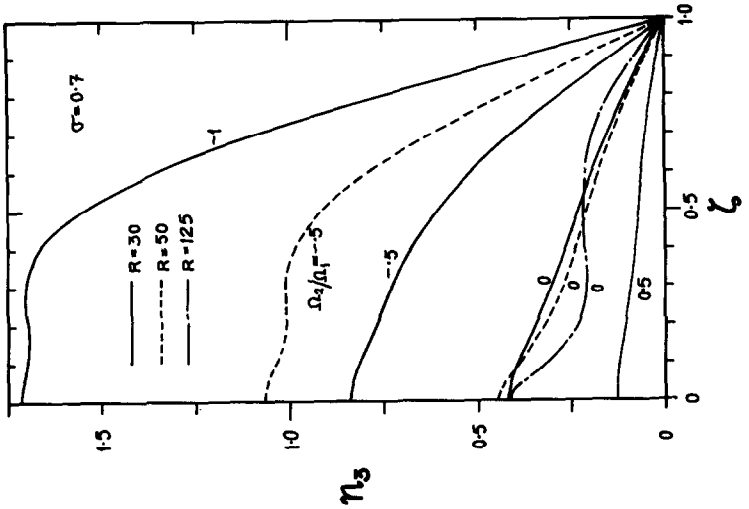

FIG. 13. Variation of the non-dimensional temperature component n_3 with ζ.

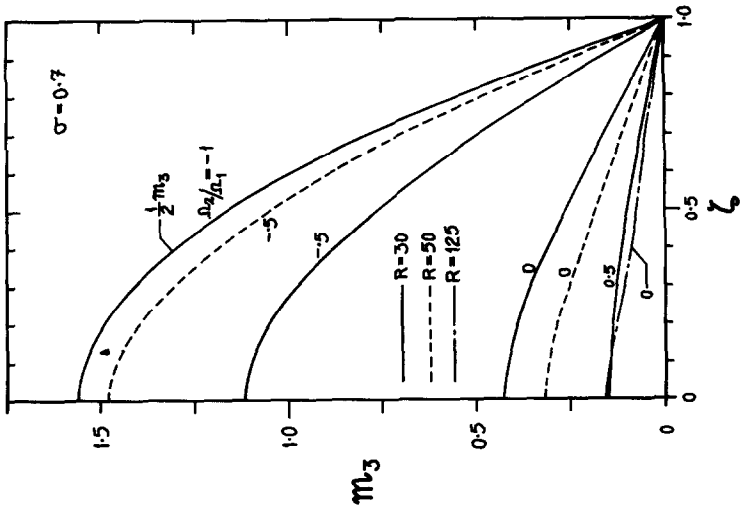

FIG. 12. Variation of the non-dimensional temperature component m_3 with ζ.

Problem 2: Here again, when $D = 1$, the solution to the equations are given by $m_3(\zeta) = n_3(\zeta) \equiv 0$, which is to be expected as the fluid is moving as a rigid body.

For the limiting case $R \to 0$, the solution is given by

$$m_3(\zeta) = \frac{\sigma}{6}(1 - D)^2[5 - 6\zeta^2 + \zeta^4]$$
$$n_3(\zeta) = \frac{\sigma}{2}(1 - D)^2[1 - \zeta^2]. \tag{30}$$

Here again, the heat transfer is by conduction only, the temperature profile being nonlinear because of dissipation.

In this problem, in the absence of dissipation, the temperature profile would be $m_3 = n_3 \equiv 0$. Thus all the temperature profiles show the effects of dissipation. The variation of m_3 and n_3 are shown in Figs. 12 and 13 respectively, and the effects of the Prandtl number on their shapes are shown in Fig. 14 for $R = 10$ and $D = 0$.

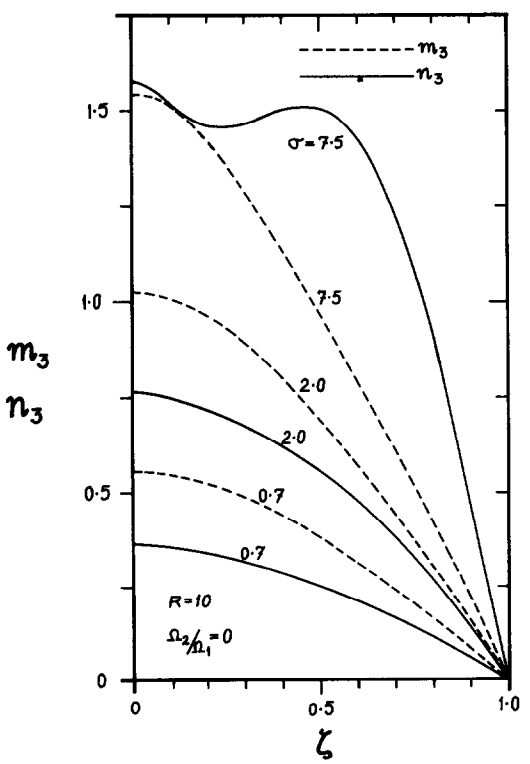

FIG. 14. Effect of the Prandtl number on the temperature components m_3 and n_3.

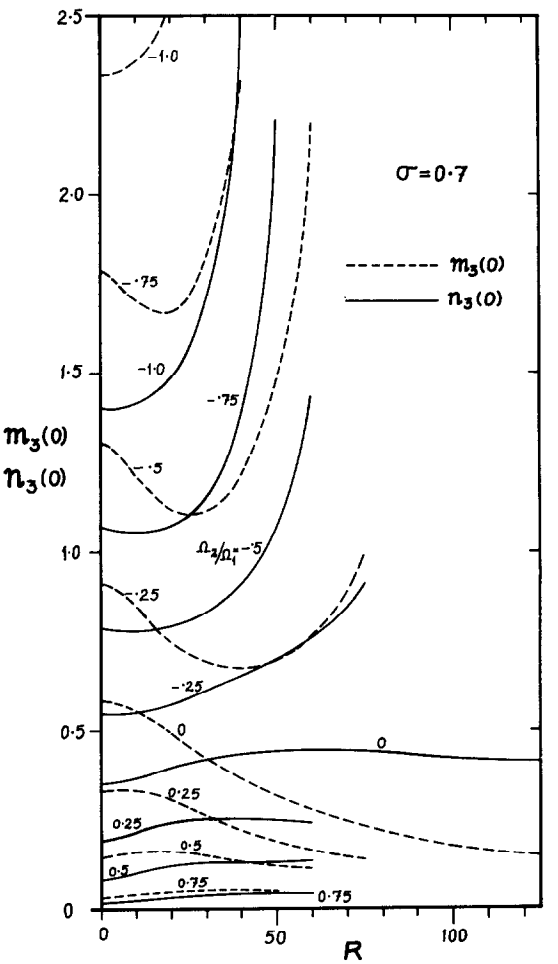

FIG. 15. Variations of the disk temperature components $m_3(0)$ and $n_3(0)$ with R.

The temperature of the insulated disk is given by $\vartheta_3(\xi, 0) = m_3(0) + \xi^2 n_3(0)$. The variations of $m_3(0)$ and $n_3(0)$ with R, for and D varying from 0·75 to −0·75, are shown in Fig. 15. The values of these quantities for $R = 0$ can be obtained from equation (30) and are given by $m_3(0) = 5\sigma(1 - D)^2/6$ and $n_3(0) = \sigma(1 - D)^2/2$.

With reference to equation (28), the heat

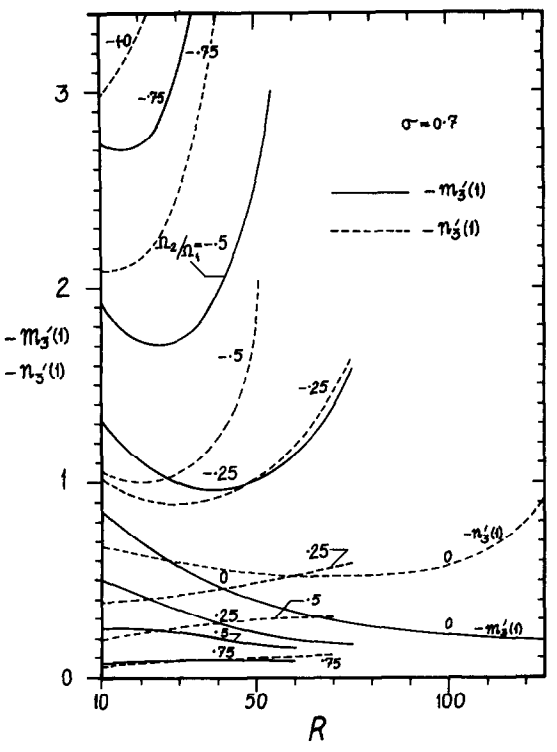

FIG. 16. Variations of the non-dimensional heat flux components $-m_3'(1)$ and $-n_3'(1)$ with R.

transfer at the upper disk can be determined in terms of $m_3'(1)$ and $n_3'(1)$. Their variations with R for $\sigma = 0{\cdot}7$ are shown in Fig. 16. As the Reynolds number is increased, $m_3(0)$ and $m_3'(1)$ decrease for $0 \leqslant D \leqslant 1$, show a minimum and then increase rapidly for $-1 < D < 0$. On the other hand $n_3(0)$ and $n_3'(1)$ increase with the Reynolds number for all values of D.

Extensive numerical data on the flow fields and on the temperature profiles, together with their graphical variation, are available in Arora [4].

REFERENCES

1. P. J. CHAPPLE and V. K. STOKES, On the flow between a rotating and a stationary disk, Report No. FLD8, Dept. of Mech. Engg., Princeton University (1962).
2. G. N. LANCE and M. H. ROGERS, The axially symmetric flow of a viscous fluid between two infinite rotating disks, *Proc. R. Soc.* **266A**, 109 (1962).
3. G. L. MELLOR, P. J. CHAPPLE and V. K. STOKES, On the flow between a rotating and a stationary disk, *J. Fluid Mech.* **31**, 95 (1968).
4. R. C. ARORA, On the heat transfer between two rotating disks, Master's Thesis, Dept. of Mech. Engng., Indian Institute of Technology, Kanpur, India (1969).
5. K. MILLSAPS and K. POHLHAUSEN, Heat transfer by laminar flow from a rotating plate, *J. Aeronaut. Sci.* **19**, 120 (1952).

TRANSFERT THERMIQUE ENTRE DEUX DISQUES TOURNANTS

Résumé—On a obtenu les solutions numériques exactes pour un écoulement permanent axisymétrique d'un fluide newtonien isovolume entre deux disques tournants parallèles et infinis, avec des rapports de vitesse des deux disques variant entre —1 et +1 par pas de 0,25 et pour des nombres de Reynolds compris entre 0 et 125. Quelques représentations graphiques adimensionnelles des vitesses radiale, tangentielle et axiale ont été données.

Ces profils de vitesse ont été utilisés pour l'intégration de l'équation de l'énergie dans deux ensembles de conditions aux limites: les deux disques sont maintenus à température constante et un disque est adiabatique tandis que l'autre est à température constante. Les solutions ont été obtenues pour des valeurs du nombre de Prandtl comprises entre 0,7 et 7,5. Les termes de dissipation n'ont pas été négligés mais les propriétés du fluide ont été supposées constantes.

Des solutions numériques exactes ont été ainsi obtenues pour le problème de transfert thermique entre deux disques.

DER WÄRMEÜBERGANG ZWISCHEN ZWEI ROTIERENDEN SCHEIBEN

Zusammenfassung—Exakte numerische Lösungen der Navier-Stokes-Gleichungen wurden erhalten für die stationäre, achsensymmetrische Strömungceiner inkompressiblen Newtonschen Flüssigkeit zwischen zwei unendlichen, rotierenden Platten bei Geschwindigkeitsverhältnissen der beiden Scheiben, die zwischen −1 und +1 in Schritten von 0.25 variieren und für Reynolds-Zahlen zwischen 0 und 125. Einige typische, dimensionslose Geschwindigkeitsprofile für die Radial-, Tangential- und Axialgeschwindigkeit sind graphisch dargestellt.

Diese Geschwindigkeitsprofile wurden dann zur Integration der Energiegleichung für zwei Arten von Randbedingungen verwendet: Einmal werden beide Scheiben auf einer konstanten Temperatur gehalten,

zum anderen ist eine Scheibe isoliert und nur die zweite wird auf konstanter Temperatur gehalten. Für einen Bereich der Prandtl-Zahl von 0,7 bis 7,5 wurden Lösungen berechnet. Der Reibungsterm ist nicht vernachlässigt, aber die Stoffwerte der Flüssigkeit werden als konstant vorausgesetzt.

Damit wurden exakte, numerische Lösungen für das Zwei-Scheiben-Wärmeübertragungsproblem

О ТЕПЛООБМЕНЕ МЕЖДУ ДВУМЯ ВРАЩАЮЩИМИСЯ ДИСКАМИ

Аннотация—Получено точное численное решение уравнений Навье-Стокса для стационарного осесимметричного течения несжимаемой ньютоновской жидкости между двумя параллельными бесконечными вращающимися дисками при отношениях скоростей от — 1 до +1 с шагом 0,25 и числах Рейнольдса от 0 до 125. Некоторые типичные безразмерные радиальные, тангенциальные и аксиальные скорости представлены графически.

Эти профили скорости использовались при интегрировании уравнения энергии для двух систем граничных условий: оба диска находятся при постоянной температуре; один диск изолирован, а температура другого постоянна. Получены решения для чисел Прандтля от 0,7 до 7,5. Членами, характеризующими диссипацию, не пренебрегали, но при этом свойства жидкости считались постоянными.

Таким образом получены численные решения задачи о теплообмене двух дисков.